PAPER • OPEN ACCESS

Using Modelica to investigate the dynamic behaviour of the German national standard for high pressure natural gas flow metering

View the article online for updates and enhancements.

Related content

IOP ebooks™

Bringing you innovative digital publishing with leading voices to create your essential collection of books in STEM research.

Start exploring the collection - download the first chapter of every title for free.

Using Modelica to investigate the dynamic behaviour of the German national standard for high pressure natural gas flow metering

M von der Heyde[1], G Schmitz[1] and B Mickan[2]

[1] Institut für Thermofluiddynamik, Hamburg University of Technology, Germany
[2] Physikalisch-Technische Bundesanstalt, Germany

E-mail: heyde@tuhh.de, schmitz@tuhh.de and bodo.mickan@ptb.de

Abstract

This paper presents a computational model written in Modelica for the high pressure piston prover (HPPP) used as the national primary standard for high pressure natural gas flow metering in Germany. With a piston prover the gas flow rate is determined by measuring the time a piston needs to displace a certain volume of gas in a cylinder. Fluctuating piston velocity during measurement can be a significant source of uncertainty if not considered in an appropriate way. The model was built to investigate measures for the reduction of this uncertainty. Validation shows a good compliance of the piston velocity in the model with measured data for certain volume flow rates. Reduction of the piston weight, variation of the start valve switching time and integration of a flow straightener were found to reduce the piston velocity fluctuations in the model significantly. The fast and cost effective generation of those results shows the strength of the used modelling approach.

Keywords: Modelica, modelling dynamic physical systems, high pressure piston prover, high pressure natural gas flow metering

(Some figures may appear in colour only in the online journal)

Nomenclature

a	Acceleration
f	Relative deviation
h	Specific enthalpy
k	Measured parameters
m	Mass
p	Static absolute pressure
s	Spatial coordinate
t	Time
u	Specific internal energy
v	Velocity
A	Cross area
F	Force
T	Temperature
V	Volume
Y	Opening function of valve
Δ	Difference, Amplitude
ρ	Density
τ	Time constant
ζ	Pressure loss coefficient

1. Introduction

Natural gas is one of the worlds most frequently used energy carriers and transported over large distances in high pressure pipelines or as liquefied natural gas using ships. For the trade with natural gas the uncertainty of the gas flow meters is of major importance. The uncertainty depends on the calibration chain and increases with every calibration step. Therefore the German national metrological institute

Physikalisch-Technische Bundesanstalt uses a high pressure piston prover as a national primary standard for the calibration of high pressure natural gas flow meters. Other primary standards for high pressure natural gas metering are for example PVTt-standards or gravimetric standards. PVTt-standards measure the pressure and temperature in a known volume to determine the mass that has flown though a transfer standard in the only inlet during a certain time. Gravimetric standards weigh the gas. International comparisons of the national standards ensure the consistency and accuracy of the measurements.

2. Modelica

Modelica is a non-proprietary, equation-based and object-oriented modelling language [1]. It can be used to assess dynamic physical systems, described as a set of ordinary differential, algebraic and discrete equations. Modelica is therefore not limited to any physical or technical domain. The first specification was published in 1997. The non-profit Modelica association is responsible for the development and publication of the Modelica language as well as the Modelica standard library. The Modelica standard library is a standardized and free library, currently consisting of 1360 models and 1280 functions from a wide range of engineering domains.

Modelica models are highly reusable because they are equation-based and object-oriented. This allows us to build on previous work, which is essential when developing complex models. For the model presented in this paper it was possible to use several components from the Modelica Standard Library containing equations from various physical domains, such as tribology, thermodynamics and fluid flow. Parts of the model, such as the medium description, are replaceable due to the object-orientation of Modelica which allows for easy modification.

As Modelica is equation-based, physical equations can be inserted in the model directly minimizing errors during the modelling process. The conversion from the physical equations to the solving algorithm is automatically done by the Compiler.

Several simulation tools based on Modelica are available. One of them is Dymola®[2], which was used to develop and evaluate the model described in this paper. It is possible in Dymola® to build up models directly in the Modelica Language and connect those models or any other model graphically.

3. High pressure piston prover

The HPPP is operated and owned by the German national metrological institute Physikalisch-Technische Bundesanstalt (PTB) and currently installed on the calibration site for gas flow meters pigsar™ in Dorsten, Germany.

The HPPP can be operated with inlet pressures up to 90 bar and flow rates up to 480 m³ h⁻¹ [3].

The central element of the HPPP is a piston in a cylinder. Indicators are mounted on the cylinder to signal the piston position. Pressure and temperature are measured downstream

of the cylinder. Some other components are needed for the calibration of transfer standards and have to be considered here as their dynamic behaviour has an effect on the piston motion, such as the transfer standards themselves, several valves and a nozzle bank.

The whole calibration set-up is shown in figure 1.

The closing of start valve 2 commences the running-in phase (start valve 1 is already open as it is only needed to prevent movement of the piston in between calibration runs due to the pressure drop across start valve 2). The motion of the piston is indicated by the piston position indicator a_1. The measurement phase starts as the piston passes indicators a_2, b_2, c_2 and ends as the piston passes the indicators a_4, b_4, c_4. The volume flow rate is determined as stated in equation (1) from the volume in between the indicators V_{PP} and the time span Δt_{PP} as given by the piston position indicator signals. It is therefore traceable to standards of length and time.

$$\dot{V}_{PP} = \frac{V_{PP}}{\Delta t_{PP}} \qquad (1)$$

Turbine meters (TM) are currently used as transfer standards. TM measure the mass flow rate using the rotational speed of a turbine inserted in the fluid flow. The rotational speed of the turbine is metered by counting magnetically induced discrete signals. The volume flow rate $\dot{V}_{TM}$ can be determined using a relationship between the number of signals per time period indicated by the TM and the volume flow rate, known from previous calibration of the TM. Two TM are connected in a row to minimize random measuring errors. The pressure at the TM is measured at their reference point and the temperature 2 diameters downstream of the TM.

The nozzle bank is used to set the flow rate. The critical nozzles are not necessary for the operation of the HPPP but provide the advantage of decoupling the calibration set-up from pressure fluctuations downstream of the nozzle bank. It consists of several critical flow nozzles in parallel connection. The pressure downstream of the nozzles is always low enough to ensure critical flow in the nozzles.

The 4-way valve is needed to revert the gas flow direction and move the piston back to its starting position after each calibration run. The check valve is used to prevent gas from flowing past the piston during the start of the reverse movement and a safety valve is included to prevent high forces on the piston at the end of the piston reverse movement.

The HPPP is further described in detail in the [3, 4] as well as the calibration facility pigsar™ [5, 6].

4. Calibration uncertainty

The result of a calibration run is the relative deviation f of the corrected volume flow rate indicated by the TM $\dot{V}_{TM}^c$ and the corrected volume flow rate indicated by the HPPP $\dot{V}_{PP}^c$ as shown in equation (2).

$$f = \frac{\dot{V}_{TM}^c - \dot{V}_{PP}^c}{\dot{V}_{PP}^c} \qquad (2)$$
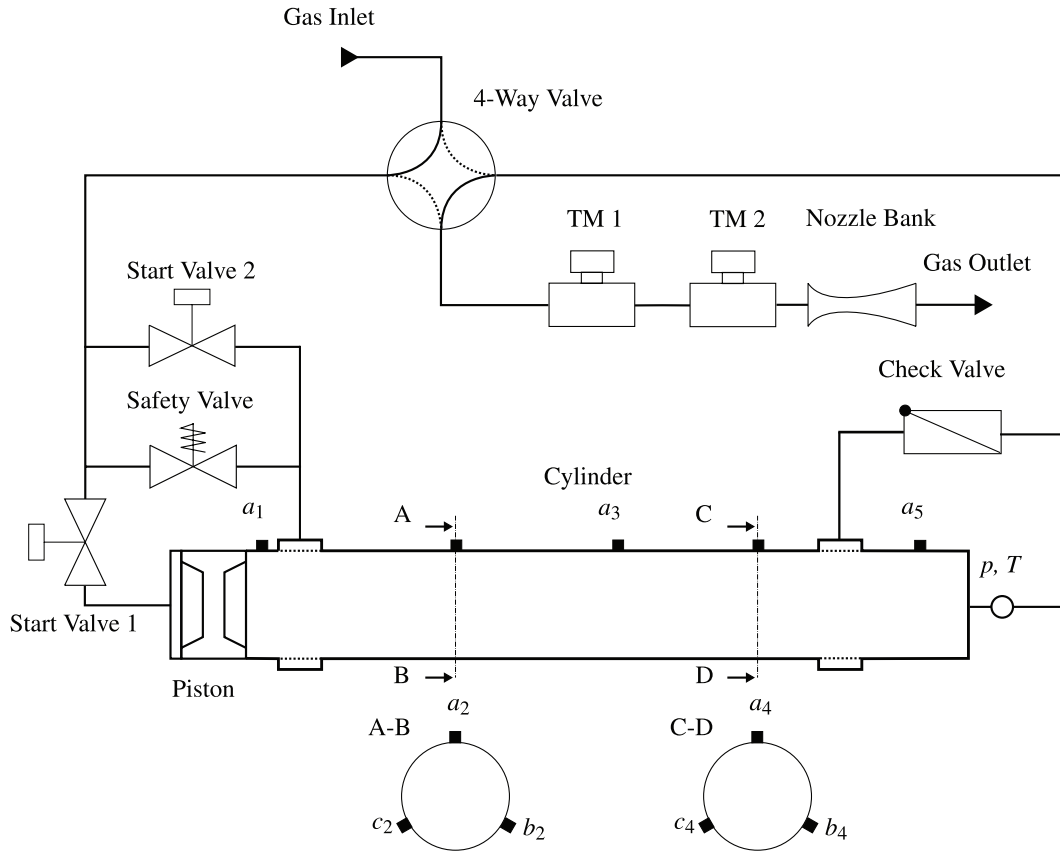
Figure 1. Scheme of the high pressure piston prover. a_1, a_5: Position Indicator. a_2, b_2, c_2: Measurement Start Indicator. a_3: Half-Way Indicator. a_4, b_4, c_4: Measurement Stop Indicator.

Several corrections are used in equation (2) to improve the calibration accuracy.

1. The volume flow rate indicated by the turbine meters $\dot{V}_{TM}$ is corrected as shown in equation (3) to prevent an error caused by the discrete nature of the TM signals. Δt_{PP} is the duration of the measurement phase as determined from the piston position indicator signals. Δt_{TM} is the time span from the first TM signal after the start of the measurement phase to the first TM signal after the end of the measurement phase.

$$\dot{V}^c_{TM} = \dot{V}_{TM}\frac{\Delta t_{PP}}{\Delta t_{TM}} \qquad (3)$$

2. The temporal mean density over the measurement phase at the piston prover $\bar{\rho}_{PP}$ and at the TM $\bar{\rho}_{TM}$, both determined from measured pressure and temperature, are used to take the density changes along the gas flow direction into account as shown in the first term of equation (4).

$$\dot{V}^c_{PP} = \dot{V}_{PP}\frac{\bar{\rho}_{PP}}{\bar{\rho}_{TM}} + \frac{V_{encl}}{\Delta t_{PP}}\frac{\rho_S - \rho_E}{\bar{\rho}_{TM}} \qquad (4)$$

3. The temporal change of the stored mass in between the cylinder and the TM during the measurement phase is taken into account as shown in the second term of equation (4), with V_{encl} being the enclosed volume, ρ_S the

spatial mean density in the enclosed volume at the start of the measurement phase and ρ_E the spatial mean density in the enclosed volume at the end of the measurement phase.

Several possible errors in the calibration process lead to the measurement uncertainty of the calibrated TM. These are

1. uncertainty in the determination of the volume in between piston position indicators,
2. uncertainty in the determination of the mean density,
3. repeatability of the TM measurement,
4. leakage between piston and cylinder,
5. dynamic error of the TM,
6. uncertainty in the determination of the stored mass in the enclosed volume.

The dynamic error of the TM is a consequence of the incorrect measurement of fast fluctuating volume flow rates due to turbine inertia. This error can be diminished using a mathematical correction method [7], but the correction method as well has uncertainties.

The resulting uncertainty of the calibrated transfer standards is 0.06% [4, 6]. The last two listed errors combined lead to an uncertainty of 0.035% [7]. They are of dynamic nature and a consequence of piston velocity fluctuations. Figure 2 shows the measured data for such piston velocity fluctuations in the measurement phase.
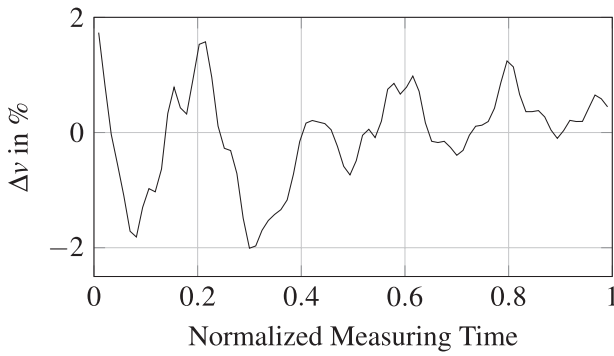
Figure 2. Relative deviation of the measured piston velocity from it's mean velocity Δv over the normalized measuring time.

The model is built to assess the dynamics of the HPPP and to find ways to reduce the piston velocity fluctuation and therefore also the measurement uncertainty of the HPPP.

5. Description of the model

A graphical representation of the model is shown in figure 3.

Several general assumptions were used in the model.

1. Pressure losses are proportional to the dynamic pressure,
2. the gas flow is one dimensional,
3. the system is adiabatic,
4. potential energy of the gas can be neglected,
5. no leakage occurs,
6. the heat transfer in the gas can be neglected in comparison to convective energy transport.

The gas at the inlet to the HPPP is assumed to have a constant temperature and pressure. This is consistent with measurement data and is modelled using a supply volume of infinite size. Equations (5) and (6) set these boundary conditions with T_{IN} being the inlet temperature and p_{IN} the inlet pressure.

$$T_{IN} = \text{const.} \qquad (5)$$

$$p_{IN} = \text{const.} \qquad (6)$$

The nozzle bank sets the other boundary condition. The used nozzles comply with ISO 9300 [8]. The nozzles are modelled using a constant critical volume flow rate $\dot{V}_N$ through all nozzles as shown in equation (7).

$$\dot{V}_N = \text{const.} \qquad (7)$$

The valves have a linear opening function $Y(t)$ and the mass flow $\dot{m}_V$ is proportional to the pressure drop across the valve Δp_V as shown in equation (8) with $\dot{m}_V^n$ and Δp_V^n being the nominal mass flow and pressure drop.

$$\dot{m}_V = \Delta p_V \frac{\dot{m}_V^n}{\Delta p_V^n} Y(t) \qquad (8)$$

The start valves are used in the model to eliminate the influence of guessed initial conditions on the piston movement, as the stationary flow condition at the beginning of the running-in phase is not known.

The HPPP is used to meter natural gas flow. Due to the high pressure and the high precision a real gas model is necessary. A Modelica implementation of GERG 2008 with a constant gas composition out of 10 molecules is used. GERG 2008 derives the equation of state for natural gas from the free energy. It is described in detail in the references [9, 10].

The enclosed gas volumes in the measuring cylinder change with piston movement. They can store mass m and internal energy mu as stated in equations (9) and (10). The volumes have i inlets or outlets. h is the specific enthalpy, v the mean velocity in a cross area A, p the static pressure and V the Volume. The pressure losses at inlets and outlets Δp are considered using constant coefficients ζ_A as shown in equation (11) with $\bar{\rho}$ being the mean density. No gradient for the thermodynamic state and no fluid friction is considered in the volumes.

$$\frac{\mathrm{d}m}{\mathrm{d}t} = \sum_{i=1}^{n} \dot{m}_i \qquad (9)$$

$$\frac{\mathrm{d}}{\mathrm{d}t}(mu) = \sum_{i=1}^{n} \dot{m}_i \left(h_i + \frac{v_i^2}{2} \right) + p\dot{V} \qquad (10)$$

$$\Delta p = \zeta_A \frac{\bar{\rho}}{2} v_A^2 \qquad (11)$$

The position of the piston is determined from the equation of motion (12) with $F_{F,P}$ being the friction force on the piston, Δp_P the pressures difference across the piston, A_P the piston cross area, m_P the piston weight and a_P the piston acceleration.

$$a_P = \begin{cases} 0 & \text{for} \quad |F_{F,P}| \geqslant |\Delta p_{PP}|A_P \\ \dfrac{\Delta p_P A_P - F_{F,P}}{m_P} & \text{for} \quad |F_{F,P}| < |\Delta p_{PP}|A_P \end{cases} \qquad (12)$$

The friction force on the piston is described as the sum of velocity independent Coulomb friction F_C, velocity proportional friction $F_P v_P$ and Stribeck friction $F_S e^{-kv_P}$ as stated in equation (13).

$$F_F = F_C + F_P v_P + F_S e^{-kv_P} \qquad (13)$$

The coulomb friction F_C is modelled as a function of the piston position s_P. This function is determined by measuring the power consumption of a linear motor moving the piston slowly through the cylinder. Measured data is only available for 80% of the cylinder length. After that the coulomb friction is assumed constant.

The velocity proportional friction F_P was determined from measuring the pressure difference across the piston for different piston velocities and by linear interpolation of the measured data points.

The pipes can store mass m, internal energy mu and momentum mv as stated in equations (14)–(16). A finite volume discretisation in the direction of fluid flow is used. Each finite volume reaches from cross area i to cross area $i + 1$. In equations (14)–(16) $\dot{m}$ is the mass flow, h the specific
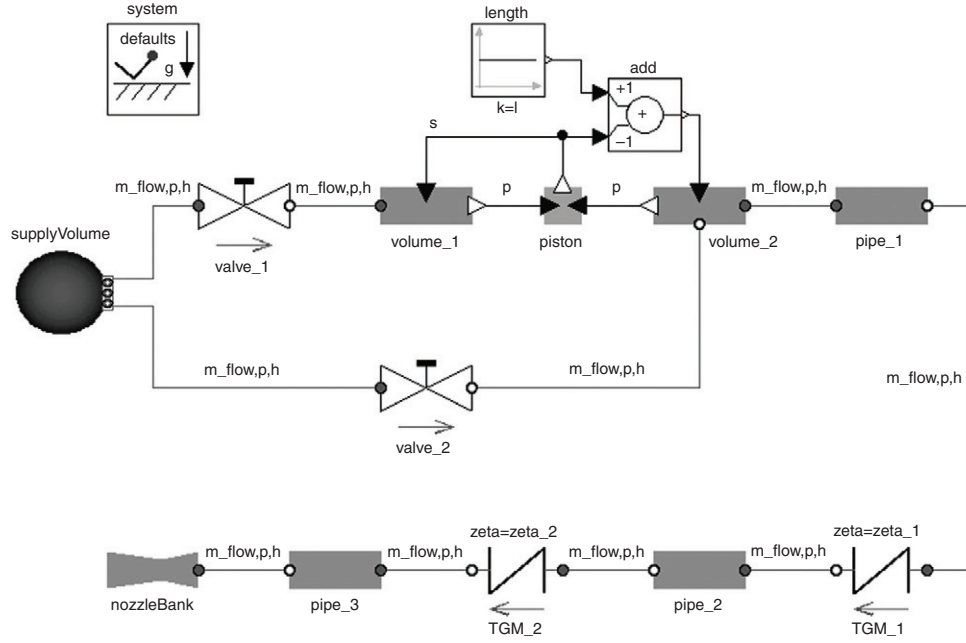
Figure 3. Graphical top-layer representation of the computational model as displayed in Dymola®.
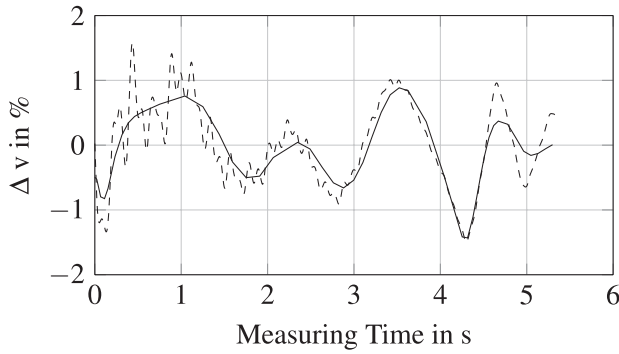
Figure 4. Relative deviation of the piston velocity from the mean velocity Δv in the model for different relative solver tolerances using Dassl. —— TOL $= 10^{-4}$, - - - - TOL $= 10^{-6}$ and TOL $= 10^{-8}$.

enthalpy, v the mean velocity, A the cross area, p the pressure and F_F the pipe friction force.

$$\frac{\mathrm{d}m}{\mathrm{d}t} = \dot{m}_i + \dot{m}_{i+1} \tag{14}$$

$$\frac{\mathrm{d}}{\mathrm{d}t}(mu) = \dot{m}_i h_i + \dot{m}_{i+1} h_{i+1} + \frac{1}{2}(vA(p_{i+1} - p_i) + vF_F) \tag{15}$$

$$\frac{\mathrm{d}}{\mathrm{d}t}(mv) = \dot{m}_i|v_i| + \dot{m}_{i+1}|v_{i+1}| - A(p_{i+1} - p_i) - F_F \tag{16}$$

The turbine meters are modelled using a constant pressure loss coefficient ζ_{TM} as stated in equation (17) with Δp_{TM} being the pressure loss, $\bar{\rho}$ the spatial mean density and v_A the mean velocity in the cross area A.

$$\Delta p_{TM} = \zeta_{TM} \frac{\bar{\rho}}{2} v_A^2 \tag{17}$$

The pressure loss coefficient ζ_{TM} is taken from measurements. The relation between the indicated volume flow rate $\dot{V}_{TM}^{\mathrm{ind}}$ and the true volume flow rate $\dot{V}_{TM}$ in the TM can be modelled as shown in equation (18) [7]. The time constant τ is modelled as stated in equation (19) using a linear relation between the time constant and the initial mass flow $\dot{m}_{IC}$ as approximately found in measurement.

$$\frac{\mathrm{d}}{\mathrm{d}t}(\dot{V}_{TM}^{\mathrm{ind}}) = \frac{\dot{V}_{TM}^{\mathrm{ind}} - \dot{V}_{TM}}{\tau} \tag{18}$$

$$\tau = k\dot{m}_{IC} \tag{19}$$

6. Verification

As measure for the verification and validation, the relative deviation of the piston velocity from it's mean velocity in the measurement phase Δv, is used. Δv represents the piston velocity fluctuations and is calculated as shown in equation (20) using the piston velocity v_P and the mean piston velocity $\bar{v}_P$ determined from the distance Δl and the duration of the measurement phase Δt. For an easy comparison of different volume flow rates a normalized time t_n is used in the figures. It is determined as in equation (21) from the time t, the start time of the measurement phase t_s and the duration of the measurement phase Δt.

$$\Delta v = \frac{v_P - \bar{v}_P}{\bar{v}_P} \quad \text{with} \quad \bar{v}_P = \frac{\Delta l}{\Delta t} \tag{20}$$
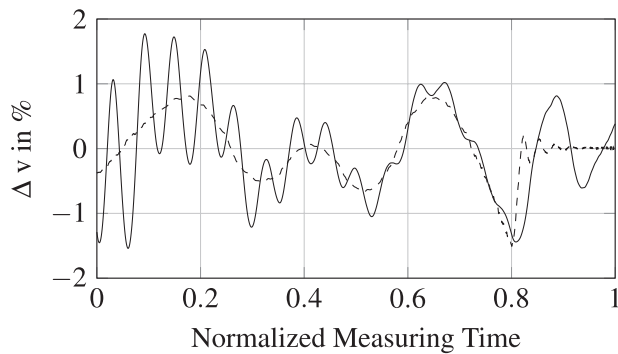
$$t_n = \frac{t - t_s}{\Delta t} \tag{21}$$

For the time-integration the Solver Dassl included in Dymola® is used with a relative tolerance of 10^{-6} [2].
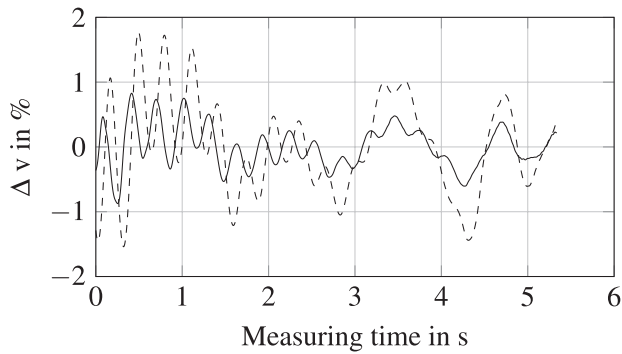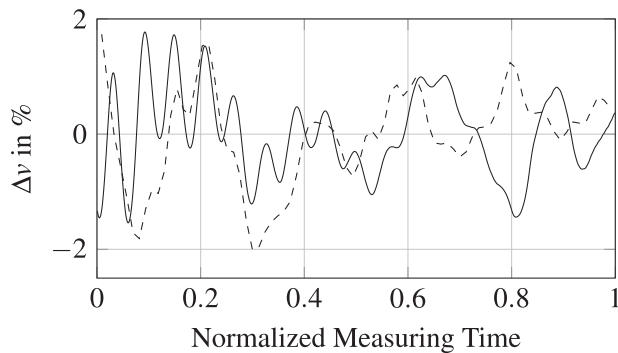
Figure 5. Relative deviation of the piston velocity from the mean velocity Δv in the model over the measuring time for different inlet pressures. —— $p_{IN} = 50$ bar. - - - - $p_{IN} = 20$ bar.

Figure 6. Relative deviation of the piston velocity from the mean velocity Δv in the model over the measuring time for different volume flow rates. —— $\dot{V}_N = 100$ m^3 h^{-1} - - - - $\dot{V}_N = 25$ m^3 h^{-1}.
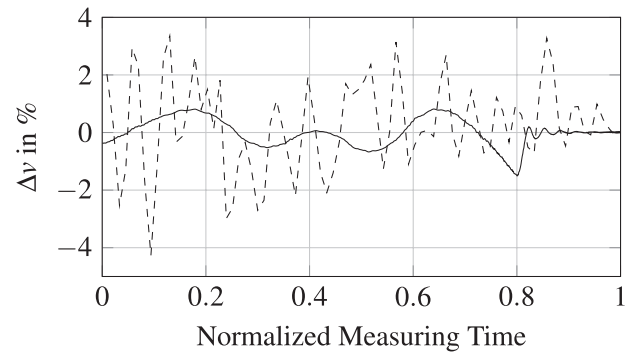

Figure 7. Comparison of the relative piston velocity deviation Δv over the normalized measuring time in the model and in measured data for a volume flow rate of 100 m^3 h^{-1} and an inlet pressure of 20 bar. —— Simulation - - - - Measurement.

A further decrease of the relative tolerance does not change the model trajectory as shown in figure 4. No major change in the trajectories is detected when using other high order variable step solvers implemented in Dymola®.

Due to calculation time constraints it is not possible to use a high number of finite pipe volumes in conjunction with real gas behaviour. Here 4 discrete volumes in the first pipe and 2 volumes in the 2nd and 3rd pipe are used.

The verification of the model shows an increasing frequency and decreasing deflection of the relative piston velocity deviation for increasing inlet pressures as shown in figure 5.

Figure 8. Comparison of the relative piston velocity deviation Δv over the normalized measuring time in the model and in measured data for a volume flow rate of 25 m^3 h^{-1} and an inlet pressure of 20 bar. —— Simulation - - - - Measurement.
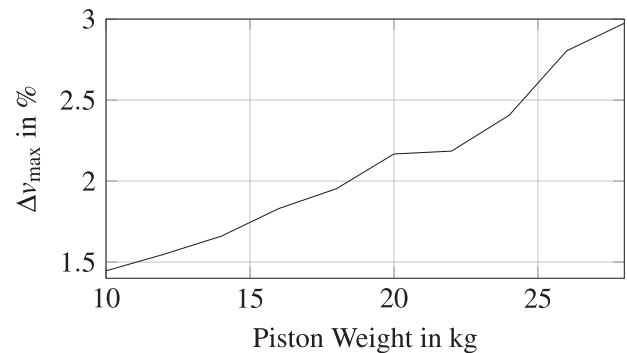
Figure 9. Maximum deviation of piston velocity from mean velocity in measuring phase for different piston weights.

Due to a shorter duration of the running-in phase, the piston velocity fluctuation resulting from piston acceleration remains active during the measuring phase for higher volume flow rates as shown in figure 6.

7. Validation

The model accuracy is highly relevant due to the low measuring uncertainty of the high pressure piston prover. It depends on the uncertainty of the measured parameters used for the calibration of the model, the mentioned general assumptions, the simplified mathematical description and the accuracy of the numerical algorithm.

Measured data for the piston velocity is used to validate the model. The piston velocity was measured for volume flow rates up to 100 m^3 h^{-1} using a laser distance measurement system.

The model validation shows relatively good accordance of the piston velocity fluctuations with measurement data for a volume flow rate of 100 m^3 h^{-1}, as shown in figure 7. The ground oscillation as well as the superimposed high frequency oscillation show similar characteristics for a volume flow rate of 100 m^3 h^{-1}. This is also valid for different inlet pressures.

For lower volume flow rates the model is not able to reproduce the measured piston velocity fluctuations. As an example the piston velocity fluctuation in the model is compared with
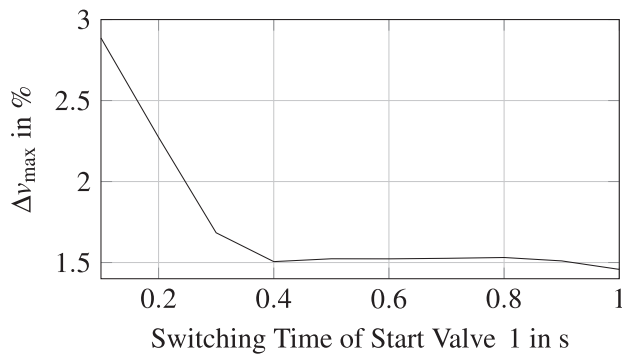
Figure 10. Maximum deviation of piston velocity from mean velocity in measuring phase for different switching times of start valve 1.
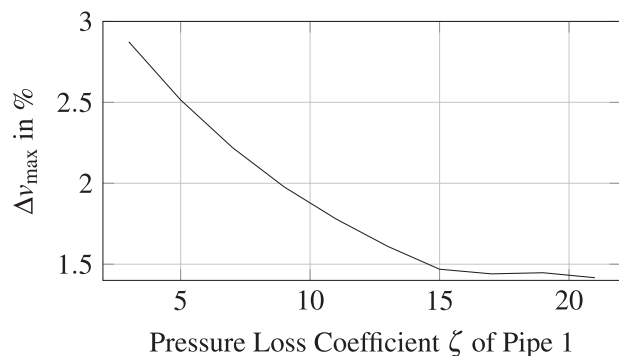
Figure 11. Maximum deviation of piston velocity from mean velocity in measuring phase for different pressure loss coefficients in pipe 1.

measurement data for a volume flow rate of $25\ m^3\,h^{-1}$ in figure 8. It can be seen, that the high frequency fluctuation in the measured data is not present in the model for a volume flow rate of $25\ m^3\,h^{-1}$.

Measuring uncertainties of the parameters used for model calibration and of the data used for validation might play an important role for low volume flow rates, as the mean velocity is lower. Also the used friction model for the piston is presumed to not be accurate enough for low volume flow rates. But as a volume flow rate of $25\ m^3\,h^{-1}$ is at the lower end of the high pressure piston prover operating area, this deficiency can be accepted.

8. Results

The model is used here to evaluate three different ways to reduce the piston velocity fluctuations in the measuring phase. The maximum deviation of the piston velocity from it's mean velocity Δv_{max} is used as a measure for the piston velocity fluctuations. The mean piston velocity deviation would not be an adequate measure, as it does not limit the important piston velocity deviation at the start and end of the measurement phase, whereas the maximum piston velocity deviation does.

The results are shown for a volume flow rate of $100\ m^3\,h^{-1}$ and an inlet pressure of 20 bar. The solver is set according to verification and validation.

Figure 9 shows the maximum relative deviation of the piston velocity from it's mean velocity in the measuring phase for different piston weights. A lower piston weight leads to lower maximum piston velocity fluctuation in the model. The real piston weight is $21.7\,kg$. Reducing the piston weight by 50% would lead to a significant drop of the piston velocity fluctuations. A way to achieve this reduction can be a change of the piston material from aluminum to fiber reinforced polymers.

Another way to reduce the piston velocity fluctuations in the model is shown in figure 10. As can be seen, the switching time of start valve 1 has a strong influence on the maximum deviation of the piston velocity from its mean velocity during the measuring phase below a switching time of 0.4 s. The switching time could be adopted to other volume flow rates using a controller.

Figure 11 shows the maximum relative deviation of the piston velocity from it's mean velocity in the measuring phase as a function of the pressure loss coefficient of pipe 1. A significant reduction of the piston velocity fluctuations can be achieved for higher pressure loss coefficients. A possibility to raise the pressure loss coefficient would be the integration of a flow straightener. The error due to a higher pressure loss between the HPPP and the TM can be avoided using correction step 2 as described in section 4.

9. Conclusions

Three independent measures to reduce the piston velocity fluctuations of the high pressure piston prover were identified using the developed model. A significant reduction of the maximum piston velocity fluctuation during the measuring phase was found achievable by lowering the piston weight, an appropriate setting of the start valve switching time and the integration of a flow straightener. These measures are expected to reduce the high pressure piston prover measuring uncertainty and can be realized with low effort.

As the computational model presented in this paper is written in Modelica, it was possible to reuse models from the Modelica Standard Library keeping the modelling time and cost low. The results show, that a modelling approach, as chosen in this work, can be very cost and time effective.

References

[1] Modelica Association 2014 Modelica specification—version 3.3 revision 1 www.modelica.org
[2] Dassault Systemes 2016 Dymola dynamic modeling laboratory user manual www.3ds.com
[3] Aschenbrenner A 1991 Prüfschein der Rohrprüfstrecke
[4] Mickan B and Kramer R 2009 PTBs metrological infrastructure for gas measurement *PTB Mitt.* **119** (special issue)
[5] Uhrig M, Schley P, Jaeschke M, Vieth D, Altfeld K and Krajcin I 2006 High precision measurement and calibration technology as a basis for correct gas billing *23rd World Gas Conf.*

[6] Mickan B, Kramer R, Müller H, Strunck V, Vieth D and Hinze H-M 2008 Highest precision for gas meter calibration worldwide: the high pressure gas calibration facility pigsar with optimized uncertainty *Int. Gas Union Research Conf.*

[7] Mickan B, Kramer R, Strunck V and Dietz T 2010 Transient response of turbine flow meters during the application at a high pressure piston prover *15th Flow Measurement Conf.*

[8] DIN EN ISO 9300:2005-11 Measurement of gas flow by means of critical flow Venturi nozzles

[9] Kunz O, Klimeck R, Wagner W and Jaeschke M 2007 The GERG 2004 wide range equation of state for natural gases and other mixtures *GERG Tech. Monogr.* **15**

[10] Kunz O and Wagner W 2012 The GERG 2008 wide range equation of state for natural gases and other mixtures *J. Chem. Eng.* **57** 3030–91